Nonlinear fractional stimulated Raman exact passage in three-level λ systems

N. Shirkhanghah[a] and M. Saadati-Niari[b,*]
[a]*Department of Physics, Khalkhal Branch, Islamic Azad University, Khalkhal, Iran.*
[b]*Department of Physics, Faculty of Sciences, University of Mohaghegh Ardabili, P.O. Box 179, Ardabil, Iran.*
[*]*e-mail: m.saadati@uma.ac.ir*

Received 2 January 2020; accepted 12 February 2020

We adapt the nonlinear stimulated Raman exact passage technique first proposed by Dorier *et al.* [*Phys. Rev. Lett.* **119** (2017) 243902] to fractional population transfer in Λ configurations and extend it to nonlinear N-pod systems. We use the nonlinear fractional stimulated Raman adiabatic passage technique in a Λ system and indicate that the nonlinear fractional stimulated Raman exact passage technique can guide the dynamics of the system as efficiently as a nonlinear fractional stimulated Raman adiabatic passage technique but with considerably smaller Rabi frequency amplitudes. We also use the nonlinear fractional stimulated Raman exact passage technique in fractional creation of ground molecular Bose-Einstein condensates from atomic Bose-Einstein condensates and show that this technique is robust against moderate variations in peak Rabi frequencies and in time delay between the pulses.

Keywords: NLF-STIREP; NLF-STIRAP; Bose-Einstein condensates.

PACS: 03.67.Lx; 32.80.Qk DOI: https://doi.org/10.31349/RevMexFis.66.344

1. Introduction

Stimulated Raman adiabatic passage (STIRAP) [2–9] is a beautifully developed and robust technique that allows the precise control of population transfer from one quantum state to another in three-level quantum systems. In this technique the Stokes pulse, linking the initially unpopulated ground state to the exited state, arrives before the pump pulse, linking the initially populated ground state to the exited state. Fractional stimulated Raman adiabatic passage (F-STIRAP) [10, 11] is a change of STIRAP, which allows the creation of any preselected coherent superposition of the two ground states in a three-level Λ system. In F-STIRAP technique, the two pulses vanish simultaneously while maintaining a constant finite ratio of amplitudes.

Coherent creation of ground molecular BECs from atomic BECs [12–19], leads to dynamics described by a nonlinear Schrödinger equation. Recently, nonlinear stimulated Raman adiabatic passage technique (NL-STIRAP) has been implemented in order to population transfer in nonlinear quantum systems [12, 14, 20, 21]. However, with similar conditions with respect to linear counterparts, the NL-STIRAP needs very large Rabi pulse areas which maybe hard to achieve experimentally [12, 14, 17].

Dorier *et al.* [22] have established a nonlinear stimulated Raman exact passage (NL-STIREP) technique using resonance-locked inverse engineering in a three-level Λ system featuring second and third order nonlinearities. In their method, there is no need for adiabatic passage conditions because the obtained solutions are exact. In comparison with NL-STIRAP -in which the population transfer efficiency is about 80%- this technique (NL-STIREP) allows an efficient and robust population transfer with Rabi pulse areas comparable to the ones of their linear counterpart. In NL-STIREP technique, the peak value of the Rabi frequency, associated to the second-order nonlinearity, is only a few times larger than its linear counterpart and the third-order nonlinearities are dynamically compensated by choosing the suitable detunings, which is considered as resonance-locked inverse engineering.

In this paper, we adapt the proposed technique in [22] to different target states in a three-level Λ system. We shoe that, the relevant design of the pulses, we reach to nonlinear fractional stimulated Raman exact passage (NLF-STIREP). In the following we study numerically robustness of the system with respect to variations in the time delay between the pulses and in the exited state decay rate. To compare the advantages of this method over other similar methods, we study the nonlinear fractional stimulated Raman adiabatic passage method (NLF-STIRAP) in a three-level Λ system and calculate the appropriate values of the Rabi frequencies and time delay between the pulses. As an example in a real physical system, we study the creation of ^{87}Rb molecules from ^{87}Rb atoms (atom-molecule Λ systems) with $(\frac{1}{2} : \frac{1}{2})$ population transfer using NLF-STIREP technique by a resonance-locked inverse engineering procedure. Then, we investigate the robustness of this technique against the variations in the intensity of the Rabi frequencies and in the time delay between the pulses. To implement NLF-STIREP technique in multi-level systems, we extend this technique to the creation of any preselected coherent superposition of the ground states in nonlinear N-pod systems (N ground states coupled to an exited state), in which the second-order nonlinearity appears only on the pump couplings. In the considered system, we impose the $N-1$ ground states, which are initially coherently superposed, are coupled to an exited state via $N-1$ pump pulses with the same time dependencies and a Stokes pulse couples the exited state to the final ground state. In order to simplify our calculations, we use the useful Morris-Shore (MS) transformation [23–25] to reduce the system with $N+1$ states to an effective three-level Λ-like system. We show that, in

multi-level quantum systems with the proper pulse design, one can create coherent superposition of all ground states with equal amplitudes.

Our paper is organized as follows. In Sec. 2, we describe NLF-STIREP technique in three-level Λ system. In Sec. 3, we implement NLF-STIRAP in three-level Λ system and compare it with NLF-STIREP. In Sec. 4, we numerically study this technique in a real atom-molecule Λ system and discuss its robustness. Finally, the conclusions and discussions are summarized in Sec. 5.

2. Nonlinear fractional stimulated Raman exact passage (NLF-STIREP) in three-level systems

2.1. The model

Consider the nonlinear three-level Λ system, which is schematically shown in Fig. 1. The excited state $|2\rangle$ is coupled to the ground states $|1\rangle$ and $|3\rangle$ with the coupling strengths denoted as Ω_P and Ω_S, respectively. Here, the subscripts P (S) stand for pump (Stokes) and $\Delta_{P,S}$ are the detunings of the fields. In the interaction picture, the Hamiltonian describing the system reads:

$$\begin{aligned}\hat{\mathcal{H}}_{nl}(t) &= \hbar(\Delta_P - i\Gamma)\hat{\Psi}_2^\dagger\hat{\Psi}_2 + \hbar(\Delta_P - \Delta_S)\hat{\Psi}_3^\dagger\hat{\Psi}_3 \\ &+ \hbar\sum_{i=1}^{3} K_i\hat{\Psi}_i^\dagger\hat{\Psi}_i + \hbar[\Omega_P(t)\hat{\Psi}_2^\dagger\hat{\Psi}_1\hat{\Psi}_1 \\ &+ \Omega_S(t)\hat{\Psi}_2^\dagger\hat{\Psi}_3 + H.c.],\end{aligned} \tag{1}$$

where Γ is introduced phenomenologically to simulate the decay of the excited state $|2\rangle$, K_i (i=1, 2, 3) are Kerr nonlinearities and $\hat{\Psi}_i^\dagger$, $\hat{\Psi}_i$ are the bosonic creation and annihilation operators for the state $|i\rangle$, respectively. In the standard mean-field treatment, the boson operators are replaced by $\bar{c_i}$ and c_i

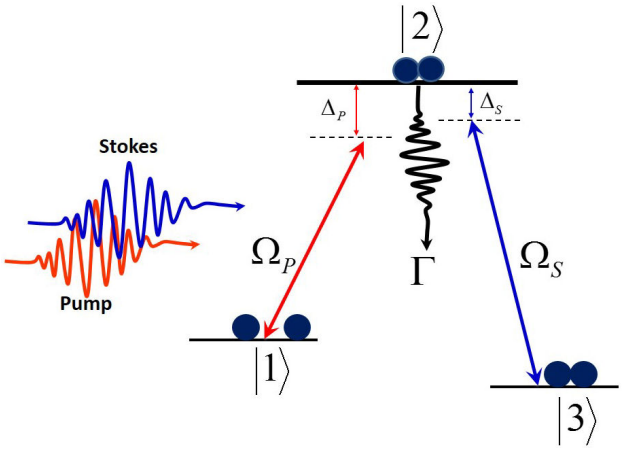

FIGURE 1. Linkage pattern scheme for the nonlinear three-level system. Ω_P, Ω_S are the coupling strengths, $\Delta_{P,S}$ are the detunings of the fields and Γ is the rate of the spontaneous emission of the excited state ($|2\rangle$) out of the system.

numbers. The mean-field approach ignores high order quantum correlations, but is expected to be valid for systems with a sufficiently large number of particles [26]. The dynamics of this system is described by the set of the mean-field coupled equations [22, 27]:

$$i\dot{c_1} = K_1c_1 + \Omega_P^*\bar{c_1}c_2, \tag{2a}$$

$$i\dot{c_2} = \Omega_Pc_1^2 + (K_2 - i\Gamma + \Delta_P)c_2 + \Omega_Sc_3, \tag{2b}$$

$$i\dot{c_3} = \Omega_S^*c_2 + (K_3 + \Delta_P - \Delta_S)c_3. \tag{2c}$$

The second-order nonlinearity appears via the pump coupling and third-order nonlinearity via the K_i terms depending on the population as follows:

$$K_i = \sum_{j=1}^{3}\lambda_{ij}|c_j|^2, \quad i = 1, 2, 3 \tag{3}$$

in which the K terms are Kerr (third-order) nonlinearities describing elastic collisions between the atom-atom, atom-molecule and molecule-molecule and λ_{ij} are constants, act like time-dependent mean-field shifts. Besides, the time-dependent c_1 and $\bar{c_1}$ terms in front of Ω_P represent the $1:2$ resonance between the atomic state and an excited molecular state. Using a change of variable $c_{2,3} \rightarrow c_{2,3}/\sqrt{2}$, we can transform the normalization condition into the usual form:

$$|c_1|^2 + |c_2|^2 + |c_3|^2 = 1. \tag{4}$$

In order to keep the mathematics as simple as possible without sacrificing generality, we neglect the nonlinear collisions between particles. Therefore, we consider the model with only second-order nonlinearities ($K_i = 0$). By choosing resonant fields ($\Delta_{P,S} = 0$) and in the absence of exited state decay ($\Gamma = 0$), the Eq. (2) is written as follows:

$$i\dot{c_1} = \Omega_P^*\bar{c_1}c_2, \tag{5a}$$

$$i\dot{c_2} = \Omega_Pc_1^2 + \Omega_Sc_3, \tag{5b}$$

$$i\dot{c_3} = \Omega_S^*c_2. \tag{5c}$$

we use general parametrization [22]:

$$c_1(t) = \cos\phi(t)\cos\theta(t), \tag{6a}$$

$$c_2(t) = -i\sin\phi(t), \tag{6b}$$

$$c_3(t) = -\cos\phi(t)\sin\theta(t), \tag{6c}$$

where $|\Psi(t)\rangle = [c_1(t), c_2(t), c_3(t)]^T$ is the state vector of system. During the time evolution of system, the angle ϕ should be near to zero to prevent the high population transfer in the state $|2\rangle$ and the mixing angle $\theta(t)$ should dynamically change from $\theta(t_i) = 0$ up to $\theta(t_f) \leq (\pi/2)$ to lead the population to the state $|3\rangle$.

Our goal is to transform the initial state of the system at time t_i, $|\Psi(t_i)\rangle$, into the state $|\Psi(t_f)\rangle$ at the end of interaction at the time t_f:

$$|\Psi(t_i)\rangle = |1\rangle, \tag{7a}$$

$$|\Psi(t_f)\rangle = c_1(t_f)|1\rangle + c_3(t_f)|3\rangle, \tag{7b}$$

where $|c_1(t_f)|^2+|c_3(t_f)|^2=1$. By adjusting $\theta(t_f)$, one can create an arbitrary coherent superposition of ground states ($|1\rangle$ and $|3\rangle$). In order to satisfy this conditions, we generalize angles of Ref. [22] as follows:

$$\theta(t)=\frac{1}{2}\eta\arcsin(|c_3(t_f)|)[1+\tanh(\frac{t}{T})], \tag{8a}$$

$$\phi(t)=\frac{4}{\pi}\epsilon\sqrt{\theta(t)\left(\frac{\pi}{2}-\theta(t)\right)}, \tag{8b}$$

where T is a normalizing time, t_f is the end of interaction time and two constants, η and ϵ, have been introduced such that allow the control of the transient population in the excited and target states. Inserting Eq. (8) into Eq. (5), we obtain the following pulses that describe Rabi frequencies satisfying the conditions of fractional population transfer in our system [22]:

$$\Omega_P(t)=\dot{\phi}\frac{1}{\cos\phi}+\dot{\theta}\frac{\tan\theta}{\sin\phi}, \tag{9a}$$

$$\Omega_S(t)=-\dot{\phi}\sin\theta+\dot{\theta}\frac{\cos\theta}{\tan\phi}. \tag{9b}$$

2.2. The numerical study

In this section, our goal is to create coherent superposition of ground states with equal amplitudes. In our method, in order to achieve coherent superposition of ground states, we choose values 0.99 and 0.1 for η and ϵ, respectively. The time delay between the two pulses (τ_0) and the pump and the Stokes Rabi frequency amplitudes (max(Ω_P), and max(Ω_S)) arise automatically from the choice of the parametrization in Eq. (8), but it does not appear explicitly in the equations. The adjustable time delay (τ) can be applied to the angles of Eq. (8) as follows:

$$\theta(t-\tau)=\frac{1}{2}\eta\arcsin(|c_3(t_f)|)\left[1+\tanh\left(\frac{t-\tau}{T}\right)\right], \tag{10a}$$

$$\phi(t-\tau)=\frac{4}{\pi}\epsilon\sqrt{\theta(t-\tau)\left(\frac{\pi}{2}-\theta(t-\tau)\right)}. \tag{10b}$$

Considering the additional time delay between pulses, the Rabi frequencies of Eq. (9) can now be written in an alternative way as follows:

$$\Omega_P(t-\tau)=\left[\dot{\phi}(t-\tau)\frac{1}{\cos\phi(t-\tau)}+\dot{\theta}(t-\tau)\frac{\tan\theta(t-\tau)}{\sin\phi(t-\tau)}\right]\chi_P, \tag{11a}$$

$$\Omega_S(t)=\left[-\dot{\phi}(t)\sin\theta(t)+\dot{\theta}(t)\frac{\cos\theta(t)}{\tan\phi(t)}\right]\chi_S, \tag{11b}$$

where two constants χ_P and χ_S have been introduced to change in the amplitude of the pump and Stokes Rabi frequencies.

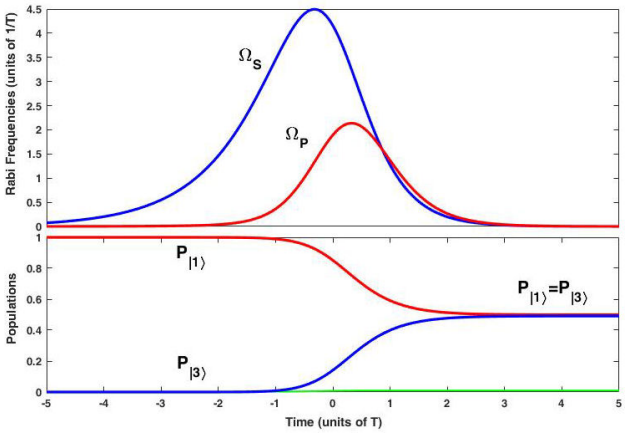

FIGURE 2. A typical example of NF-STIREP which leads to a coherent superposition of ground states with equal amplitudes for $\epsilon=0.1$, $\eta=0.99$, $\tau=0$, $\Gamma=0$, $\tau_0=0.64T$, and $\chi_{P,S}=1$. Top frame: Stokes and pump Rabi frequencies, determined by Eq. (11). Bottom frame: Time evolution of the populations.

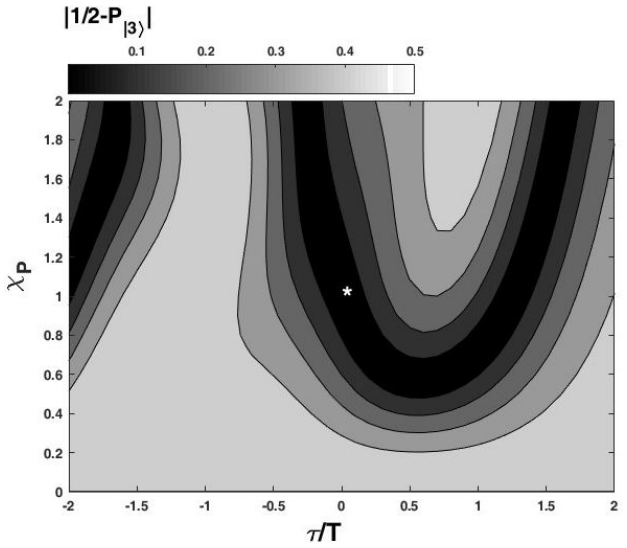

FIGURE 3. Contour plot at the final time t_f of $|(1/2)-P_{|3\rangle}|$ as function of time delay between the pulses (τ) and to the pump pulse Rabi frequency amplitude coefficient (χ_P) with $\chi_S=1$, in a nonlinear three-level system. Other parameters are as in Fig. 2. The figure represents the robustness of the nonlinear fractional stimulated Raman exact passage in this system. The white star points to the exact solution of the inverse engineering, depicted in Fig. 2.

Figure 2 represents an example of NLF-STIREP which leads to a coherent superposition of ground states with equal amplitudes $\left(|c_1(t_f)|^2=|c_3(t_f)|^2=(1/2)\right)$. In the top panel, we plot the corresponding Rabi frequency of the pulses and in the low frame, we show the dynamics of the populations. The Rabi frequencies have a simple and standard form close to Gaussian pulses and similar to the F-STIRAP, the two pulses vanish simultaneously while maintaining finite ratio of amplitudes. The main feature in the procedure of control is its stability with respect to changes in the physical parameters of the system. Therefore, in the following we

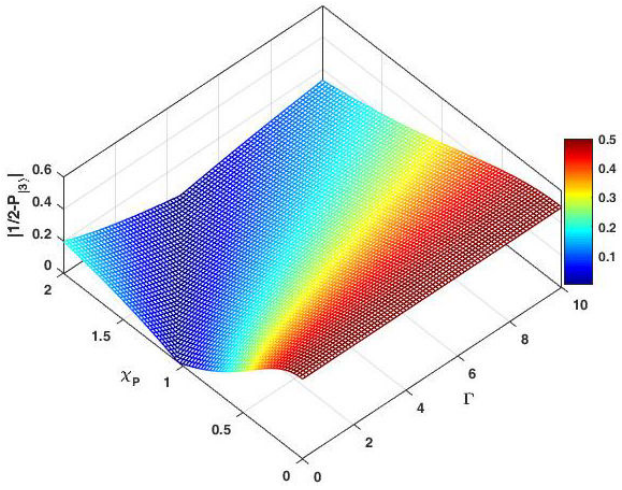

FIGURE 4. The final population of $|(1/2) - P_{|3\rangle}|$ as function of the decay rate of the unstable state $|2\rangle$ (Γ) and to the pump pulse Rabi frequency amplitude coefficient (χ_P) with $\chi_S = 1$, in a nonlinear three-level system. The figure represents the robustness of the nonlinear fractional stimulated Raman exact passage in this system. Other parameters are as in Fig. 2.

study these changes and investigate their effects on the robustness of the system. In Fig. 3, the final population $|(1/2) - P_{|3\rangle}|$ is plotted against the time delay between the pulses τ and to the pump amplitude coefficient (χ_P) for a fixed Stokes peak coefficient ($\chi_S T = 1$). For sufficiently strong laser pulses, there is an optimal range of τ in which $|(1/2) - P_{|3\rangle}| = 0$ is most easily achieved. For example, for a $\chi_S T = 1$ and $0.7 \geq \chi_P T \geq 0.5$, acceptable range is $0.15 \leq \tau \leq 0.9$. As shown in Fig. 3, this system is robust with respect to variations of τ and χ_P. Considering the exited state decay (Γ), the efficiency of population transfer in our system is reduced. In Fig. 4, the final population $|(1/2) - P_{|3\rangle}|$ is plotted against the exited state decay rate Γ and to the pump Rabi frequency amplitude coefficient, for a fixed Stokes Rabi frequency amplitude coefficient ($\chi_S = 1$). According to the figure, for $\Gamma = 0$ this diagram is in the full agreement with Fig. 2 for a $\chi_P T = 1$, but with the growing of Γ, in order to achieve fractional population transfer with equal amplitudes ($|(1/2) - P_{|3\rangle}| = 0$), we must increase the pump Rabi frequency amplitude coefficient. This system is robust with respect to small variations in the exited state decay Γ, however for sufficiently high decay rates, the efficiency of population transfer decreases considerably.

3. Nonlinear fractional stimulated Raman adiabatic passage (NLF-STIRAP) in three-level systems

We consider a nonlinear three-level Λ system, depicted in Fig. 1, where $|1\rangle$ represents an atomic state and $|2\rangle$, $|3\rangle$ are the excited and ground diatomic molecular states, respectively. Existence of a coherent population trapping (CPT) state with zero eigenenergy in coupled atom-molecule systems has been reported in several recent experiments [16]. If our system initially prepared in a CPT state, it will stay in the instantaneous CPT state. This is the adiabatic theorem generalized to this nonlinear system. In general, nonlinear systems, because of collisions and intrinsic quantum fluctuations, dynamically unstable regimes appear for the CPT state and adiabaticity will therefore break down [28]. Nevertheless, in our current work, we assume that the system under consideration is always dynamically stable. Setting $c_2 = 0$ in Eq. (5b) and combining it with the total particle number conservation ($|c_1^0|^2 + |c_3^0|^2 = 1$) leads to the following CPT population distribution:

$$|c_1^0|^2 = \frac{2}{1 + \sqrt{1 + 4\left(\frac{\Omega_P^2}{\Omega_S^2}\right)}} = 1 - |c_3^0|^2, \tag{12a}$$

$$|\text{CPT}\rangle = \mathcal{N}[\Omega_S|1\rangle - |c_1^0|\Omega_P|3\rangle], \tag{12b}$$

where $\mathcal{N}$ is normalization factor and $|\mathbf{\Psi}_0(t)\rangle = [c_1^0, c_2^0, c_3^0]^T$ is the corresponding state vector of system in CPT state. In order to achieve fractional population transfer with equal amplitudes in this system, we impose $\Omega_S(t_f) = |c_1^0(t_f)|\Omega_P(t_f)$ in the CPT stat (Eq. (12b)). Using Eq. (12) and after the simple algebra yields:

$$\tan\beta = \frac{\Omega_P}{\Omega_S} = \sqrt{2}, \tag{13}$$

where β is a mixing angle. Without loss of generality, we assume that the coupling strengths $\Omega_{P,S}$ are real and positive. We use three equal-amplitude Gaussian pulses, a pump pulse and two Stokes pulses first with the same time dependence as the pump pulse and latter coming earlier as follows [29]:

$$\Omega_P(t) = \Omega^0 \sin(\beta) \exp\left[-\frac{(t-\tau)^2}{T^2}\right], \tag{14a}$$

$$\Omega_S(t) = \Omega^0 \exp\left[-\frac{(t+\tau)^2}{T^2}\right] + \Omega^0 \cos(\beta) \exp\left[-\frac{(t-\tau)^2}{T^2}\right], \tag{14b}$$

where T is the duration of each pulse, and τ is the time delay between the pulses. A typical example of time evolution in NLF-STIRAP is shown in Fig. 5. The pulse shapes are defined by Eq. (14) with $\tau = 0.64T$, $\Omega_0 T = 20$ and $\beta = \arctan(\sqrt{2})$. The population evolves from state $|1\rangle$ (ground state) to the coherent superposition $(1/\sqrt{2})(|1\rangle + |3\rangle)$, very similar to the standard F-STIRAP. Comparing Fig. 2 and Fig. 5, we find out, the NLF-STIREP technique can guide the dynamics of the system as efficiently as a NLF-STIRAP, but with considerably smaller Rabi frequency amplitudes. For example in the NLF-STIRAP, $\Omega_0 \approx (20/T)$ is required to get about the same high transfer efficiency to the target states and low transient population to the exited state as NLF-STIREP with $\Omega_P^{\max} \approx (2/T)$ and $\Omega_S^{\max} \approx (4.5/T)$.

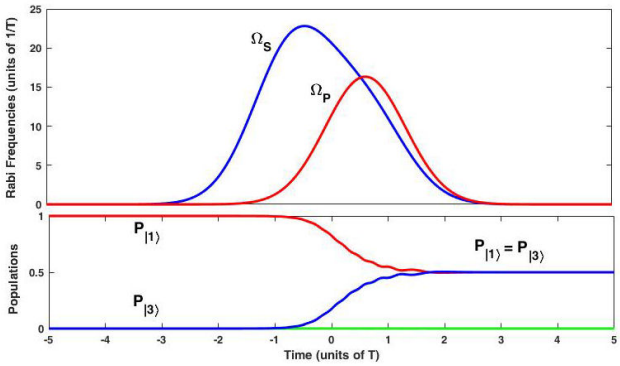

FIGURE 5. A typical example of NLF-STIRAP in three-level system in the resonance case ($\Delta = 0$) for $\tau = 0.64T$, $\Omega_0 T = 20$, and $\beta = \arctan(\sqrt{2})$. Upper : Stokes and pump Rabi frequencies, determined by Eq. (14). Lower : Time evolution of the populations that leads to coherent superposition of atomic and molecular ground states with final equal amplitudes.

4. Nonlinear fractional stimulated Raman exact passage (NLF-STIREP) in a real physical system

In order to perform a numerical study in a real physical system, we consider a pair of ^{87}Rb atoms in state $|1\rangle$ wich is photoassociated by a pump laser field of molecular Rabi frequency $\Omega_P^{'}(t)$ into a molecule in exited state $|2\rangle$, which is subsequently driven into a ground molecular state $|3\rangle$ by a Stokes laser field of molecular Rabi frequency $\Omega_S^{'}(t)$. The nonlinear collisions between particles are important in the ultracold quantum atomic or molecular systems (atomic BECs and ground molecular BECs) [30–32]. Here, we use Eq. (2) for this system with considering third-order nonlinearities (K_i) and off-resonant fields ($\Delta_{P,S} \neq 0$) in the presence of the exited state decay (Γ) in which, $\Omega_P(t) = \Omega_P^{'}(t)\sqrt{n}$, $\Omega_S(t) = \Omega_S^{'}(t)$, and n is condensate density [33]. Since the Kerr nonlinearities cause unstable regions in the parameter space [15, 34], to avoid it, we have to consider the phase $\gamma(t)$ in Eq. (6) as follows:

$$c_1(t) \Longrightarrow c_1(t)e^{-i\gamma(t)}, \quad c_{2,3}(t) \Longrightarrow c_{2,3}(t)e^{-2i\gamma(t)}. \quad (15)$$

We see that setting $\dot{\gamma} = K_1$ and using resonance locking conditions [22], one can rewrite Eq. (2) as Eq. (5) with the inclusion of exited state decay where, Kerr terms have been compensated by detunings. Our goal is to show that, the NLF-STIREP technique can be implemented in the ultracold quantum atomic or molecular systems to transfer the population from the atomic condensate directly to the molecular condensate with equal amplitudes using counterintuitively ordered pump and Stokes pulses [see Eq. (11)]. Our results can be best understood with reference to Table I which gives the values of typical NLF-STIREP with $((1/2) : (1/2)$ population transfer parameters characteristic of a condensate of ^{87}Rb atoms [13, 35]. Using the values of the parameters in Table I, and an optimum values $\epsilon = 0.1$, $\eta = 0.99$, we can achieve almost 98% efficiency of fractional conversion of atomic BECs into molecular BECs, even including the exited state ($|2\rangle$) spontaneous emission [see Fig. 6]. In this figure, the atom-ground molecule conversion efficiency is defined as fraction of the initial number of atoms converted into molecules as follows:

$$\zeta = \frac{2n_3(\infty)}{n_1(0)}, \quad (16)$$

where n_1 is the initial number of atoms and $n_3(\infty)$ is the final number of molecules. Figure 7 represents the final pop-

TABLE I. Typical parameter values and mean-field interaction potentials for efficient fractional stimulated Raman exact passage in rubidium condensates.

Γ	3.7×10^7 s^{-1}	Decay of the quasibound molecule.
T	3.1×10^{-5} s	Pulse duration.
χ_P	250	Coefficient of pump Rabi frequency amplitude.
χ_S	250	Coefficient of Stokes Rabi frequency amplitude.
λ_{11}	21328 s^{-1}	Atom-atom elastic interactions.
λ_{33}	10664 s^{-1}	Molecule-molecule elastic interactions.
$\lambda_{13} = \lambda_{31}$	-27692 s^{-1}	Atom-molecule elastic interactions.
λ_{2i}	0	Other elastic interactions.
n	4.3×10^{20} m^{-3}	Condensate density.

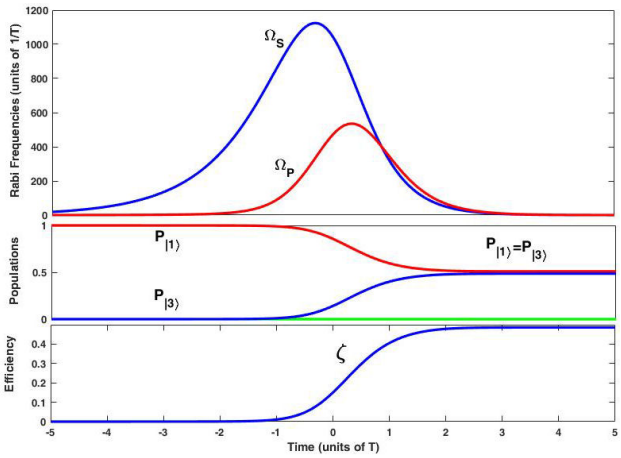

FIGURE 6. NLF-STIREP in ^{87}Rb atom-molecule Λ system for $\epsilon = 0.1$, $\eta = 0.99$, $\tau = 0$, and $\tau_0 = .64T$. Other parameters are defined in Table I. Upper : Stokes and pump Rabi frequencies, determined by Eq. (11). Middle : Time evolution of the populations that leads to coherent superposition of atomic and molecular ground states with equal amplitudes. Lower : Time evolution of conversion efficiency ζ (16).

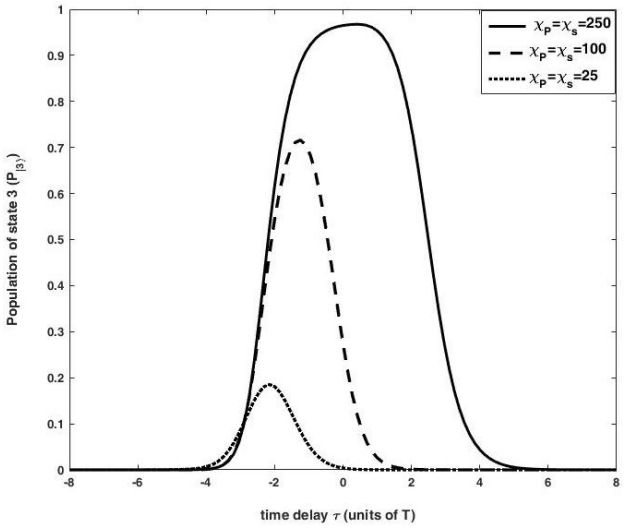

FIGURE 7. The final population $P_{|3\rangle}$ as function of time delay between the pulses for NLF-STIREP in ^{87}Rb atom-molecule Λ-system with $\epsilon = 0.1$, $\eta = 0.99$ for $\chi_P = \chi_S = 250$, $\chi_P = \chi_S = 100$, and $\chi_P = \chi_S = 25$, respectively.

ulation $P_{|3\rangle}$ as function of time delay between the pulses (τ) with $\epsilon = 0.1$, $\eta = 0.99$. Other parameter values are as in Table I. This figure shows that NLF-STIREP technique is robust against moderate variations of in the time delay between pulses, but the efficiency of population transfer decreases considerably by reducing the coefficient of Rabi frequency amplitudes. For instance, with $|\tau| \leq 0.7T$ and $\chi_P = \chi_S = 250$ the efficiency of fractional conversion from atomic BECs into molecular BECs is approximately 98%, but with a decrease in the coefficient of Rabi frequency amplitudes down to $\chi_P = \chi_S = 25$, conversion efficiency also declines to 18%. However, the obtained solutions are exact and there is no need for adiabatic conditions, but the adiabatic passage conditions still exist ($\chi_P T, \chi_S T \gg 1$).

5. Conclusion and discussion

We can generalize, in principle, our approach to the nonlinear N-pod systems. This opens up the search for new schemes for various configurations based on NLF-STIREP and NLF-STIRAP. Figure 8a) features the linkage pattern of these systems, where $N-1$ ground states, which are initially coherently superposed, are coupled to an excited state via $N-1$ pump pulses with the same time dependencies and a Stokes pulse couples the excited state to the final ground state. Without taking into consideration of the Kerr terms (third-order nonlinearity) and the exited state decay, the second-order nonlinearity appears only on the pump couplings. Following the MS transformation, one can then find a basis that decouples $N-2$ ground states from the others [36–38] [see Fig. 8b)]. If the initial state is coherently superposed, using

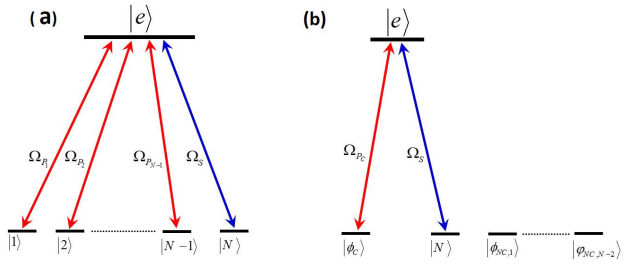

FIGURE 8. (a) Linkage pattern of the nonlinear N-pod system. (b) Linkage pattern of the nonlinear N-pod system in the MS basis.

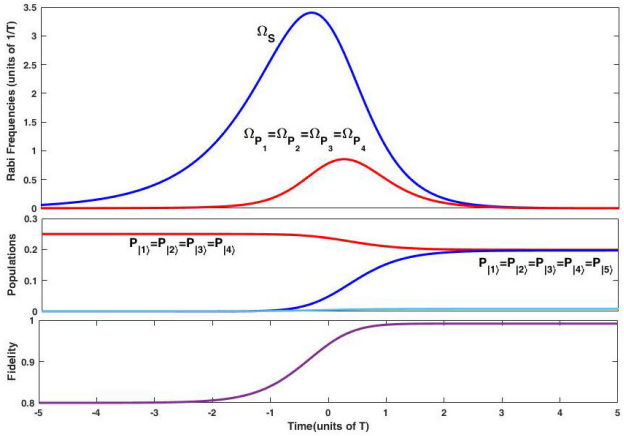

FIGURE 9. NLF-STIREP in a penta-pod system ($N = 5$) with $\epsilon = .1$, $\eta = .99$, $\tau = 0$, $\Gamma = 0$, $\tau_0 = 0.64T$, and $\chi_{P,S} = 1$. Upper : Stokes and pump Rabi frequencies, determined by Eq. (17). Middle : Time evolution of the populations that lead to the coherent superposition of ground states with equal amplitudes. Lower : Dynamics of the fidelity of the desired state ((19b)).

the following pulses, one can create coherent superposition of all ground states with equal amplitudes.

$$\Omega_{P_i}(t) = \dot{\phi}\frac{1}{\cos\phi} + \dot{\theta}\frac{\tan\theta}{\sin\phi}, \quad i = 1, 2, 3, \ldots, N-1 \tag{17a}$$

$$\Omega_S(t) = -\dot{\phi}\sin\theta + \dot{\theta}\frac{\cos\theta}{\tan\phi}, \tag{17b}$$

where

$$\theta(t) = \frac{1}{2}\eta \arcsin\left(\sqrt{\frac{1}{N}}\right)\left[1 + \tanh\left(\frac{t}{T}\right)\right], \tag{18a}$$

$$\phi(t) = \frac{4\epsilon}{\pi}\sqrt{\theta\left(\frac{\pi}{2} - \theta\right)}. \tag{18b}$$

Figure 9 shows an example of such a superposition in nonlinear penta-pod system with equal amplitudes in which, all applied pulses are on exact resonance with their transitions. The initial and final states of the system are:

$$|\Psi(t_i)\rangle = \frac{1}{\sqrt{4}}\left[|1\rangle + |2\rangle + |3\rangle + |4\rangle\right], \tag{19a}$$

$$|\Psi(t_f)\rangle = \frac{1}{\sqrt{5}}\left[|1\rangle + |2\rangle + |3\rangle + |4\rangle + |5\rangle\right]. \tag{19b}$$

In conclusion, we have studied fractional population transfer in nonlinear three-level Λ systems using the NLF-STIREP and NLF-STIRAP techniques. We have calculated numerically with the appropriate design of Rabi frequencies, one can then achieve population transfer from an initial state to a desired superposition of all ground states. We have also shown numerically, our system is robust with respect to the exited state decay. However, for sufficiently high decay rates, the efficiency of population transfer decreases considerably. Using numerical comparison, we have shown that the population transfer efficiency in the NLF-STIREP technique can be as efficiently as a NLF-STIRAP, but with considerably smaller Rabi frequency amplitudes. We have used the NLF-STIREP technique to convert the ^{87}Rb atoms into the ^{87}Rb molecules fractionally. We have shown that, with the proper and effective values of time delay between the pulses and Rabi frequency amplitudes, efficiency of fractional converting atomic BECs into molecular BECs is approximately 98%. Although, the efficiency of population transfer significantly decreases by decreasing the laser pulse amplitudes and increasing the time delay between the pulses.

Acknowledgments

We wish to acknowledge the financial support of University of Mohaghegh Ardabili.

1. U. Gaubatz, P. Rudecki, S. Schiemann, and K. Bergmann, Population transfer between molecular vibrational levels by stimulated Raman scattering with partially overlapping laser fields. A new concept and experimental results, *J. Chem. Phys.* **92** (1990) 5363, https://doi.org/10.1063/1.458514.
2. K. Bergmann, H. Theuer, and B. W. Shore, Coherent population transfer among quantum states of atoms and molecules, R*ev. Mod. Phys.* **70** (1998) 1003, https://doi.org/10.1103/RevModPhys.70.1003.
3. N. V. Vitanov, M. Fleischhauer, B. W. Shore, and K. Bergmann, Coherent Manipulation of Atoms Molecules By Sequential Laser Pulses, *Adv. At. Mol. Opt. Phys*. **46** (2001) 55, https://doi.org/10.1016/S1049-250X(01)80063-X.
4. N. V. Vitanov, T. Halfmann, B. W. Shore, and K. Bergmann, Laser-Induced Population Transfer by Adiabatic Passage Techniques, *Annu. Rev. Phys. Chem*. **52** (2001) 763, https://doi.org/10.1146/annurev.physchem.52.1.763.
5. K. Bergmann, N. V. Vitanov, and B. W. Shore, Perspective: Stimulated Raman adiabatic passage: The status after 25 years, *J. Chem. Phys.* **142** (2015) 170901, https://doi.org/10.1063/1.4916903.
6. R. G. Unanyan, Robust population transfer in atomic beams induced by Doppler shifts, *Appl. Phys. B* **122** (2016) 264, https://doi.org/10.1007/s00340-016-6538-1.
7. N. V. Vitanov, A. A. Rangelov, B. W. Shore, and K. Bergmann, Stimulated Raman adiabatic passage in physics, chemistry, and beyond, *Rev. Mod. Phys*. **89** (2017) 015006, https://doi.org/10.1103/RevModPhys.89.015006.
8. Y. A. Sharaby, A. Joshi, and S. S. Hassan, Coherent population tranfer in V-type atomic system, *J. Nonlinear Opt. Phys. Mater*. **22** (2013) 1350044, https://doi.org/10.1142/S0218863513500446.
9. W. Huang, B. W. Shore, A. Rangelov, and E. Kyoseva, Adiabatic following for a threestate quantum state, *Opt. Commun.* **382** (2017) 196, https://doi.org/10.1016/j.optcom.2016.07.067.
10. P. Marte, P. Zoller, and J. L. Hall, Coherent atomic mirrors and beam splitters by adiabatic passage in multilevel systems, *Phys. Rev. A* **44** (1991) R4118(R), https://doi.org/10.1103/PhysRevA.44.R4118.
11. N. V. Vitanov, K.-A. Suominen, and B. W. Shore, Creation of coherent atomic superpositions by fractional stimulated Raman adiabatic passage, *J. Phys. B* **32** (1999) 4535, https://doi.org/10.1088/0953-4075/32/18/312.
12. M. Mackie, R. Kowalski, and J. Javanainen, Bose-Stimulated Raman Adiabatic Passage in Photoassociation, *Phys. Rev. Lett.* **84** (2000) 3803, https://doi.org/10.1103/PhysRevLett.84.3803.
13. R. Wynar, R. S. Freeland, D. J. Han, C. Ryu, and D. J. Hainzen, Molecules in a Bose- Einstein Condensate, *Science* **287** (2000) 1016, https://doi.org/10.1126/science.287.5455.1016.
14. P. D. Drummond, K. V. Kheruntsyan, D. J. Heinzen, and R. H. Wynar, Stimulated Raman adiabatic passage from an atomic to a molecular Bose-Einstein condensate, *Phys. Rev. A* **65** (2002) 063619, https://doi.org/10.1103/PhysRevA.65.063619.
15. H. Y. Ling, H. Pu, and B. Seaman, Creating a Stable Molecular Condensate Using a Generalized Raman Adiabatic Passage Scheme, *Phys. Rev. Lett.* **93** (2004) 250403, https://doi.org/10.1103/PhysRevLett.93.250403.
16. K. Winkler, G. Thalhammer, M. Theis, H. Ritsch, R. Grimm, and J. Hecker Denschlag, Atom-Molecule Dark States in a Bose-Einstein Condensate, *Phys. Rev. Lett*. **95** (2005) 063202, https://doi.org/10.1103/PhysRevLett.95.063202.
17. A. P. Itin and S. Watanabe, Integrability, Stability, and Adiabaticity in Nonlinear Stimulated Raman Adiabatic Passage, *Phys. Rev. Lett*. **99** (2007) 223903, https://doi.org/10.1103/PhysRevLett.99.223903.
18. L. D. Carr, D. DeMille, R. V. Krems, and J. Ye, Cold and ultracold molecules: science, technology and applications, *New J. Phys.* **11** (2009) 055049, https://doi.org/10.1088/1367-2630/11/5/055049.
19. J. Zhai, L. Zhang, K. Zhang, J. Qian, and W. Zhang, Efficiency limitation for realizing an atom-molecule adiabatic transfer based on a chainwise system, *J. Opt. Soc. Am. B* **32** (2015) 2164, https://doi.org/10.1364/JOSAB.32.002164.

20. H. Jing, F. Zheng, Y. Jiang, and Z. Geng, Adiabatic condition for coherent atom- heteronuclear-molecule conversion, *Phys. Rev. A* **78** (2008) 033617, https://doi.org/10.1103/PhysRevA.78.033617.
21. S.-Y. Meng, L.-B. Fu, and J. Kiu, Adiabatic evolution for the ^{87}Rb atom-molecule conversion system, *J. Phys. B* **42** (2009) 185301, https://doi.org/10.1088/0953-4075/42/18/185301.
22. V. Dorier, M. Gevorgyan, A. Ishkhanyan, C. Leroy, H. R. Jauslin, and GuÃ©rin, Nonlinear Stimulated Raman Exact Passage by Resonancle-Locked Inverse Engineering, *Phys. Rev. Lett.* **119** (2017) 243902, https://doi.org/10.1103/PhysRevLett.119.243902.
23. J. R. Morris and B. W. Shore, Reduction of degenerate two-level excitation to independent two-state systems, *Phys. Rev. A* **27** (1983) 906, https://doi.org/10.1103/PhysRevA.27.906.
24. A. A. Rangelov, N. V. Vitanov, and B. W. Shore, Extension of the Morris-Shore transformation to multilevel ladders, *Phy. Rev. A* **74** (2006) 053402, https://doi.org/10.1103/PhysRevA.74.053402.
25. B. W. Shore, Two-state behavior in N-state quantum systems: The Morris-Shore transformation reviewed, *J. Mod. Opt*. **61** (2014) 787, https://doi.org/10.1080/09500340.2013.837205.
26. M. Mackie, R. Kowalski, and J. Javanainen, Bose-Stimulated Raman Adiabatic Passage in Photoassociation, *Phys. Rev. Lett.* **84** (2000) 3803, https://doi.org/10.1103/PhysRevLett.84.3803.
27. H. Pu, P. Maenner, W. Zhang, and H. Y. Ling, Adiabatic Condition for Nonlinear Systems, *Phys. Rev. Lett*. **98** (2007) 050406, https://doi.org/10.1103/PhysRevLett.98.050406.
28. B. Wu and Q. Niu, Nonlinear Landau-Zener tunneling, *Phys. Rev. A* **61** (2000) 023402, https://doi.org/10.1103/PhysRevA.61.023402.
29. N. V. Vitanov, K.-A. Suominen, and B. W. Shore, Creation of coherent atomic superpositions by fractional stimulated Raman adiabatic passage, *J. Phys. B* **32** (1999) 4535, https://doi.org/10.1088/0953-4075/32/18/312.
30. J. Söding, D. Guéry-Odelin, P. Desbiolles, F. Chevy, H. Inamori, and J. Dalibard, Threebody decay of a rubidium Bose-Einstein condensate, *Appl. Phys. B* **69** (1999) 257, https://doi.org/10.1007/s003400050805.
31. J. Kobayashi, Y. Izumi, K. Enomoto, M. Kumakura, and Y. Takahashi, Spinor molecule in atomic Bose-Einstein condensate, *Appl. Phys. B* **95** (2009) 37, https://doi.org/10.1007/s00340-008-3307-9.
32. L.-B. Chen, C.-H. Zheng, H.-Y. Ma, and C.-J. Shan, Robust entangling two distant Bose-Einstein condensates via adiabatic passage, *Opt. Commun*. **328** (2014) 73, https://doi.org/10.1016/j.optcom.2014.04.056.
33. H. Y. Ling, P. Maenner, W. Zhang, and H. Pu, Adiabatic theorem for a condensate system in an atom-molecule dark state, *Phys. Rev. A* **75** (2007) 033615, https://doi.org/10.1103/PhysRevA.75.033615.
34. P. Buonsante, R. Franzosi, and V. Penna, Dynamical Instability in a Trimeric Chain of Interacting Bose-Einstein Condensates, *Phys. Rev. Lett.* **90** (2003) 050404, https://doi.org/10.1103/PhysRevLett.90.050404.
35. D. J. Heinzen, R. Wynar, P. D. Drummond, and K. V. Kheruntsyan, Superchemistry: Dynamics of Coupled Atomic and Molecular Bose-Einstein Condensates, *Phys. Rev. Lett.* **84** (2000) 5029, https://doi.org/10.1103/PhysRevLett.84.5029.
36. M. Amniat-Talab, M. Saadati-Niari, S. Guérin, and R. Nader-Ali, Superposition of states by adiabatic passage in N-pod systems, *Phys. Rev. A* **83** (2011) 013817, https://doi.org/10.1103/PhysRevA.83.013817.
37. M. Amniat-Talab, M. Saadati-Niari, and S. Guérin, Quantum state engineering in iontraps via adiabatic passage, *Eur. Phys. J. D* **66** (2012) 216, https://doi.org/10.1140/epjd/e2012-30249-3.
38. B. Rousseaux, S. Guérin, and N. V. Vitanov, Arbitrary qudit gates by adiabatic passage, *Phys. Rev. A* **87** (2013) 032328, https://doi.org/10.1103/PhysRevA.87.032328.